INSTITUTE OF PHYSICS PUBLISHING JOURNAL OF PHYSICS B: ATOMIC, MOLECULAR AND OPTICAL PHYSICS

J. Phys. B: At. Mol. Opt. Phys. **39** (2006) 2849–2860 doi:10.1088/0953-4075/39/12/018

Low-energy electron collisions with C_2 using the *R*-matrix method

Gabriela Halmová, J D Gorfinkiel[1] and Jonathan Tennyson

Department of Physics and Astronomy, University College London, Gower St., London WC1E 6BT, UK

Received 17 March 2006, in final form 12 May 2006
Published 5 June 2006
Online at stacks.iop.org/JPhysB/39/2849

Abstract

Calculations are presented for the bound and continuum states of the C_2^- system using the polyatomic version of the UK molecular *R*-matrix code. The calculations, based on a 26-state close-coupling expansion, show the presence of three bound doublet states of C_2^- and a quartet state that only becomes bound at large internuclear separation. A number of resonance states are found and their behaviour as a function of the C_2 bond length is studied. Cross sections for electron impact electronic excitation are presented with particular emphasis on excitation of the d $^3\Pi_g$ state which is responsible for the well-known Swan emission bands.

(Some figures in this article are in colour only in the electronic version)

1. Introduction

The C_2 molecule is the smallest carbon chain and its spectrum is well known from cometary tails, the interstellar medium and the atmospheres of cool carbon stars. C_2 is abundant in flames and electric discharges through carbon-containing materials. Recently, the study of C_2 has become of particular interest because of the (possible) use of graphite walls in fusion devices (Fantz and Balden 2005, Stark *et al* 2005). A knowledge of electron collision cross sections is important for this and other applications. However, there appear to be no previous published studies of electron collisions with neutral C_2. This would seem to be in contrast with the C_2^- ion for which a number of studies performed using the ASTRID storage ring are available (Andersen *et al* 1996, Pedersen *et al* 1998, 1999).

Theoretically, one of the challenges of studying electron collisions with C_2 is the unusually large number of low-lying electronic states of the system which are themselves difficult to represent using standard *ab initio* methods (Abrams and Sherrill 2004). Furthermore, the C_2^-

[1] Present address: Department of Physics and Astronomy, The Open University, Walton Hall, MK7 6AA Milton Keynes, UK.

system supports several bound states although the precise number is not firmly established (Gorfinkiel *et al* 2005).

In this work, we report comprehensive calculations on the bound and continuum states of C_2^- as a function of internuclear separation. We couple the lowest 26 singlet and triplet target states, all of which lie less than 9 eV above the ground state at the C_2 equilibrium geometry. This is a significantly larger number of physical states than have been needed to obtain stable results for electron collision with other molecules studied previously using a standard close-coupled expansion. Preliminary results of this study were reported by Gorfinkiel *et al* (2005), although the calculations reported below used improved orbitals compared to the previous study.

2. Method

The *R*-matrix theory is based on dividing coordinate space into two regions using a spherical boundary centred on the centre-of-mass of the target molecule (Burke and Berrington 1993, Burke and Tennyson 2005). The position of the boundary is chosen so that the inner region contains all the electronic cloud of the target molecular states included in the calculation.

Inside the *R*-matrix sphere it is necessary to consider all short-range interactions between the N target electrons and the scattering one, such as exchange and electron correlation. In the outer region, these effects are negligible so the scattering electron can be described as moving in the long-range multipole potential of the target molecule.

The accuracy of this method is strongly dependent on the representation of the problem in the inner region (Tennyson 1996). The basis state wavefunctions for an N+1 electrons system in this region are expanded in the following way,

$$\psi_k^{N+1} = \mathcal{A} \sum_{ij} a_{ijk} \Phi_i(\mathbf{x}_1 \dots \mathbf{x}_N) u_{ij}(\mathbf{x}_{N+1}) + \sum_i b_{ik} \chi_i(\mathbf{x}_1 \dots \mathbf{x}_{N+1}) \tag{1}$$

where k represents the kth solution of the inner region Hamiltonian, $\mathcal{A}$ is the anti-symmetrization operator, $\mathbf{x}_i$ are the spatial and spin coordinates of the i electron, u_{ij} are continuum orbitals which represent the scattering electron (Tennyson and Morgan 1999), a_{ijk} and b_{ik} are variational coefficients, Φ_i is the target wavefunctions of the ith target state and χ_i are L^2 functions constructed from the target occupied and virtual molecular orbitals. These functions represent the electron-correlation and polarization effects. In first summation, the configuration state functions are constrained to give the correct (target) space and spin symmetry at the N-electron level as well as the correct total, $N + 1$ electron space spin symmetry. Doing this requires special consideration of phase effects due to electron ordering in the wavefunction (Tennyson 1997).

In this work we decided to use the UK polyatomic *R*-matrix code (Morgan *et al* 1997). This is because our long-term aim is to study electron collision with C_2^- using the newly developed molecular *R*-matrix with pseudostates (MRMPS) method (Gorfinkiel and Tennyson 2004). So far this method has been implemented only as part of the polyatomic code. The highest symmetry available in the polyatomic code is D_{2h} which is a subgroup of the true $D_{\infty h}$ symmetry of C_2. All calculations presented are performed in D_{2h} symmetry. In the polyatomic suite both target and continuum orbitals are represented by a linear combination of Gaussian-type orbitals (GTOs). The target wavefunctions are expanded as a linear combination of the configurations ϕ_k,

$$\Phi_i(\mathbf{x}_1 \dots \mathbf{x}_N) = \sum_k c_{ik} \phi_k(\mathbf{x}_1 \dots \mathbf{x}_N) \tag{2}$$

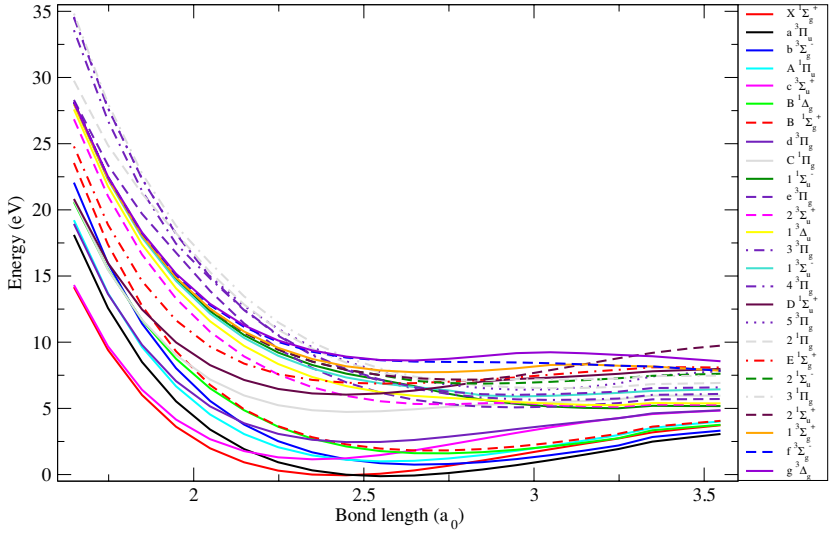

Figure 1. Potential energy curves for the 26 states of C_2 used in the calculations.

where the c_{ik} coefficients are determined by diagonalizing the Hamiltonian of the molecular target. The ϕ_k are constructed in terms of an orthonormal set of molecular orbitals. The quality of the target wavefunctions is dependent on the size of this expansion, as is indirectly, the quality of the scattering calculation (Tennyson 1996).

After the inner region wavefunctions are obtained, the *R*-matrix is computed on the boundary and propagated (Morgan 1984) to large scattering electron–target distances where it is matched to analytical expressions (Noble and Nesbet 1984). The matching gives *K*-matrices which are diagonalized to yield the eigenphase sum, and used to determine *T*-matrices from which we obtain the cross sections. For bound states a searching algorithm (see below) is used to find solutions with the correct boundary conditions.

3. Calculations

3.1. Target representation

To obtain the potential curves, calculations were performed at a series of C_2 fixed internuclear separations. Within the Born–Oppenheimer approximation these fixed calculations can be used as the input for solving nuclear problems on the underlying curves.

Fixed-nuclei calculations were performed for 20 C_2 internuclear distances in the range of 1.648 a_0 to 3.548 a_0 (with 0.1 a_0 step). The measured equilibrium geometry for the ground state is 2.348 a_0 (Huber and Herzberg 1979). Various scattering models have been tested, the largest of which comprised the 26 (in $D_{\infty h}$ symmetry or 39 in D_{2h} symmetry) target states shown in figure 1.

In order to determine the target electronic wavefunctions and energies, we first performed a Hartree–Fock self-consistent field (HF-SCF) calculation using the double-zeta plus polarization (DZP) Gaussian basis set of (Dunning 1970) for C. We used the molecular orbitals generated this way to obtain pseudo-natural orbitals (NOs). These are obtained by diagonalizing the first-order density matrix for all target states included in the calculation. To obtain a set of NOs that gives a good representation of the 26 target states included in

Table 1. C_2 adiabatic excitation energies obtained from our CASCI target calculations compared with those from an MRCI calculation, an CI calculation and experiment. Excitation energies, T_e, are given in eV. R_e are the internuclear separations for equilibrium geometry in a_0.

	CASCI		MRCI[a]		CI[c]		Observation	
Models	T_e (eV)	R_e (a_0)	T_e (eV)	R_e (a_0)	T_e (eV)	R_e (a_0)	T_e (eV)	R_e (a_0)
a $^3\Pi_u$	−0.066	2.548	0.099	2.477	−0.03	2.53	0.089[a]	2.479[a]
b $^3\Sigma_g^-$	0.809	2.648	0.804	2.595	0.80	2.65	0.798[a]	2.587[a]
A $^1\Pi_u$	1.052	2.548	1.076	2.500	1.14	2.53	1.040[a]	2.491[a]
c $^3\Sigma_u^+$	1.206	2.348	1.178	2.285	1.09	2.32	1.131[a]	2.283[a]
B $^1\Delta_g$	1.662	2.748	1.521	2.627	1.59	2.66	1.498[a]	2.617[a]
B' $^1\Sigma_g^+$	1.879	2.648	1.922	2.612	1.81	2.66	1.910[a]	2.602[a]
d $^3\Pi_g$	2.507	2.448	2.531	2.400	2.47	2.44	2.483[a]	2.392[a]
C $^1\Pi_g$	4.789	2.448	4.388	2.379	4.81	2.40	4.248[a]	2.372[a]
1 $^1\Sigma_u^-$	5.067	2.948	4.961	3.258				
e $^3\Pi_g$	5.135	2.948			5.51	3.17	5.058[b]	2.901[b]
2 $^3\Sigma_u^+$	5.182	3.248						
1 $^3\Delta_u$	5.291	3.248	5.098	3.262				
3 $^3\Pi_g$	5.693	3.048			6.47	3.00		
1 $^3\Sigma_u^-$	5.953	2.948						
4 $^3\Pi_g$	6.079	2.948						
D $^1\Sigma_u^+$	6.092	2.448			6.23	2.38	5.361[b]	2.339[b]
5 $^3\Pi_g$	6.472	2.948						
2 $^1\Pi_g$	6.581	3.048						
E $^1\Sigma_g^+$	6.928	2.548			7.18	2.46	6.823[b]	2.368[b]
2 $^1\Sigma_u^-$	6.930	2.848			7.92	3.00		
3 $^1\Pi_g$	7.128	2.748						
2 $^1\Sigma_u^+$	7.225	2.848						
1 $^3\Sigma_g^+$	7.788	2.648						
f $^3\Sigma_g^-$	–	–					8.809[b]	2.632[b]
g $^3\Delta_g$	8.678	2.648					9.074[b]	2.566[b]

[a] Boggio-Pasqua *et al* (2000).
[b] Huber and Herzberg (1979).
[c] Kirby and Liu (1979).

the close-coupling expansion, we performed a weighted average of their density matrices. Large singles and doubles configuration interaction (CISD) calculations (using around 70 000 and 110 000 configurations for the singlet and triplet states respectively) were performed to obtain the matrices. After a number of tests the best results (i.e. the best threshold energies) were obtained when 13 states—^1A_g (2 states), $^3B_{2u}$,$^3B_{3u}$, $^3B_{1g}$ (2 states), $^1B_{2u}$, $^1B_{3u}$,$^3B_{1u}$ (2 states), $^1B_{1g}$,^3A_u,^3A_g—were averaged with weights 20, 5, 20, 20, 15, 5, 10, 10, 5, 20, 5, 20, 5 respectively. We used the same state-averaging procedure for all molecular geometries.

Finally, a complete active space configuration interaction (CASCI) calculation, which built all the possible configurations by distributing the electrons among the orbitals in the active space, was performed. In this model the four 1s electrons were frozen in the $1\sigma_g$ and $1\sigma_u$ orbitals, and the remaining eight electrons were freely distributed among the $2\sigma_g$, $3\sigma_g$, $2\sigma_u$, $3\sigma_u$, $1\pi_u$ and $1\pi_g$ orbitals giving configurations which can be written as $(1\sigma_g\ 1\sigma_u)^4$ $(2\sigma_g\ 3\sigma_g\ 2\sigma_u\ 3\sigma_u\ 1\pi_u\ 1\pi_g)^8$.

The ground state $\left(X^1\Sigma_g^+\right)$ energy obtained for our equilibrium geometry $R_e = 2.448a_0$ is $-75.554\,48E_h$ in comparison with the value from full CI calculation of Christiansen *et al* (1996),$-75.730\,209E_h$ for their $R_e = 2.348a_0$. Table 1 shows the energy differences

between the ground and excited states and compares them with multi-reference CI (MRCI) calculations (Boggio-Pasqua *et al* 2000), Slater orbital CI calculations (Kirby and Liu 1979) and experimental data.

In our calculation, as in the C_2 curves constructed from constants in Huber and Herzberg (1979) (see figure in (Jones *et al* 1980)), the ground state and the first excited state (a $^3\Pi_u$) cross as a function of internuclear separation, R. In our calculations this crossing occurs near $R = 2.5a_0$ which is comparable with the results of Rosmus and Werner (1984). Our calculations find that the a $^3\Pi_u$ state lies 0.066 eV lower than the X $^2\Sigma_g^+$ state at $R = 2.548a_0$; Kirby and Liu (1979) find it is 0.03 eV lower. This energy difference is smaller than the accuracy we can hope for with the electronic structure method we use, which is in turn constrained by the need to use this calculation as part of a scattering study.

For other excitation energies the agreement with previous data, where available, can be considered good. Table 1 does not give our values for the f $^3\Sigma_g^-$ state since we find this state to be purely repulsive. In the case of the highest lying excited state included in the close-coupling expansion (g $^3\Delta_g$), our calculations suggest that this state has a double minimum. Our adiabatic excitation energy of 8.678 eV corresponds to a minimum at $R = 2.648a_0$, whereas the observed value we quote (Herzberg *et al* 1969) is for a much larger bond length; we find a local maximum in the curve at $R = 3.048a_0$ after which the energy of the curve decreases up to the last geometry we consider, at $R = 3.548a_0$.

3.2. Scattering model

The scattered electron was described by continuum orbitals which were represented by GTOs with $l \leqslant 4$ centred at the dicarbon centre of mass. As part of our preliminary study (Gorfinkiel *et al* 2005), various R-matrix radii, a, and continuum basis sets were tested. The eigenphase sums showed good agreement between the various models, so the best one ($a = 10a_0$ and the basis of Faure *et al* (2002)) was used for the present calculations. As part of this work we tested three different models for the scattering calculation. The first included in the close-coupling expansion the 15 lowest electronic states of C_2, the second included the 26 lowest states (all those shown in table 1) and third included 26 states in inner region and 15 in outer. All tests were performed for C_2 at its equilibrium bond length.

Resonance positions and widths were determined by fitting the eigenphase sum to a Breit–Wigner profile (Tennyson and Noble 1984). Eigenphases were obtained by propagating the R-matrix to $100a_0$. For the lower energy resonances, i.e. the ones discussed in this work, the differences between 15-, 26-state and mixed models is slight; results reported below are for the 26-state model.

Bound state energies were obtained using the method described by Sarpal *et al* (1991). In this method, the eigenvalue problem is reduced to finding the roots of a determinant, which depend on the energy of the system. A Gailitis expansion was applied at a radius of $30a_0$ and then the wavefunctions propagated inwards to the R-matrix boundary. The 15-state and mixed models showed better results for $^2\Sigma_g^+$ symmetry than the 26-state model. The results in table 2 are for the 15-state model which do not differ from the mixed one. We note that these bound state studies, unlike the scattering ones, require calculation of the wavefunction in the outer region. This makes the calculations numerically sensitive to the inclusion of very strongly closed channels in the outer region. As a test we also computed bound state energies simply by diagonalizing a Hamiltonian based on inner region wavefunction (1). This gave energies very similar, but slightly (less than 0.01 eV) higher, to those reported here.

Table 2. Bound states of C_2^- from various methods and observation compared with our calculations. IP is ionization potential for the ground state and T_e is the adiabatic excitation threshold for the excited states.

	$X\,^2\Sigma_g^+$		$A\,^2\Pi_u$		$B\,^2\Sigma_u^+$	
	R_e (a_0)	IP (eV)	R_e (a_0)	T_e (eV)	R_e (a_0)	T_e (eV)
MRD-CI[a]	2.415	∼3.4	2.491	0.403	2.309	2.335
MCSCF[b]	2.411	∼3.3	2.491	0.435	2.326	2.348
QCISD[c]	2.414	2.74				
CCSD[d]	2.394	3.09	2.470	0.553	2.309	2.453
Observation[e]	2.397	∼3.4[g]	2.471[f]	0.494[f]	2.312	2.280
This work	2.448	3.26	2.548	0.557	2.348	2.355

[a] Zeitz *et al* (1979).
[b] Rosmus and Werner (1984).
[c] Wang *et al* (2001).
[d] Watts and Bartlett (1992).
[e] Huber and Herzberg (1979).
[f] Rehfuss *et al* (1988).
[g] Jones *et al* (1980).

4. Results

In this section we present results on the resonance positions and widths and the bound states of C_2^-. Our calculations, which were performed for 16 symmetries and 20 geometries, yield a large amount of data, not all of which can be presented below. Because one aim of our work is to determine bound state wavefunctions of C_2^- in preparation for performing electron collision studies with this anion, we made a careful analysis of these bound states which can be compared with other works.

4.1. Bound states

We found three bound states of C_2^- of symmetry $X\,^2\Sigma_g^+$, $A\,^2\Pi_u$ and $B\,^2\Sigma_u^+$. Their energies are shown in table 2 and compared with other calculations and experiment. The agreement can be considered good. The $X\,^2\Sigma_g^+$ and $B\,^2\Sigma_u^+$ bound state potential energy curves are shown in figure 2 along with the energies of resonances of the same symmetry. Our calculations find, somewhat unusually, that the $B\,^2\Sigma_u^+$ bound state becomes a resonance in the region between 2.648 and $3.348a_0$.

All the bound states of C_2^- from our calculations are of doublet spin symmetry. However, Bondybey and Brus (1975) also reported the observation of a $^4\Sigma_u^+$ bound state. Our calculations suggest (figure 4) that at short R this state is a low-lying resonance which only becomes a bound state for $R > 3.1a_0$. Since the Bondybey and Brus' spectra were recorded in a Noble gas matrix, it is possible that matrix effects could have led to this state becoming bound.

4.2. Resonances

Autodetaching resonance states of C_2^- have been observed experimentally (Hefter *et al* 1983, Jones *et al* 1980). However, these resonances are all associated with vibrational excited states of the bound C_2^- electronic states discussed above, which have sufficient energy to autodetach. In this work we are concerned not with such nuclear excited Feshbach resonances, but resonance state associated with electronic states of C_2^- which lie in the continuum.

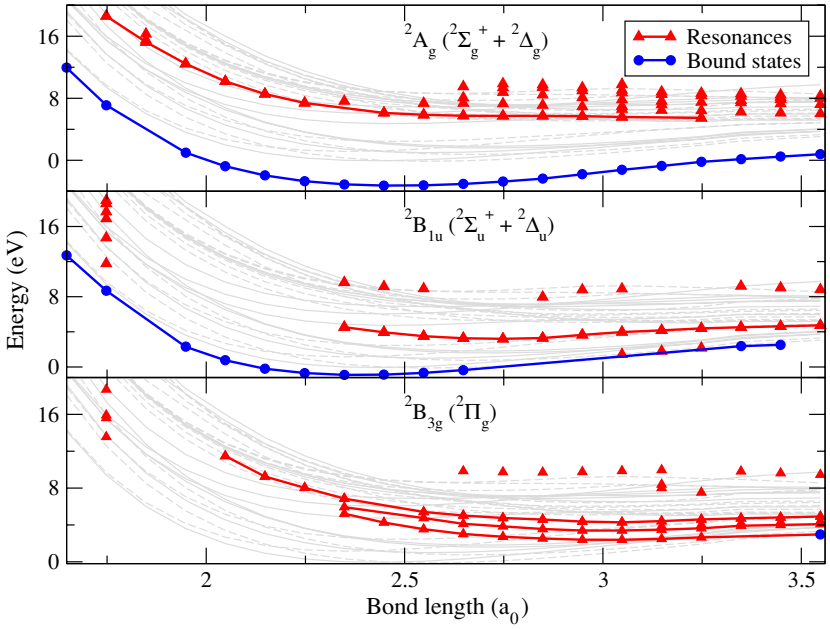

Figure 2. C_2^- bound state and resonance energies for ^2A_g ($^2\Sigma_g^+ + {}^2\Delta_g$), $^2B_{1u}$ ($^2\Sigma_u^+ + {}^2\Delta_u$) and $^2B_{3g}$ ($^2\Pi_g$) symmetries as a function of the bond length. The energies of the C_2 electronic states used in our calculations are shown in the background: singlet states as solid lines, triplet states as dashed lines.

The vertical ionization energy of C_2 is about 14.8 eV (Wang *et al* 2001). As we get energetically closer to this threshold, large (infinite) numbers of very diffuse electronically excited states are present. For this reason our scattering calculations concentrated on energies below about 10 eV. Our calculations identified many resonances. However, the density of C_2 target states made it difficult to study systematically the behaviour of these as a function of internuclear separation. This is due to the difficulty of fitting resonances which lie very close to a target state and the possibility of a resonance disappearing when it crosses a target state. We therefore concentrate on the low-lying resonances which are, in any case, probably the most important ones for problems concerned with thermal or quasi-thermal electron collisions. Data for resonances which appeared in our calculations at energies above 10 eV (such as those with $^2\Pi_u$ symmetry) will not be reported as they cannot be considered reliable.

The resonance energies for ^2A_g $\left(^2\Sigma_g^+ + {}^2\Delta_g\right)$, $^2B_{1u}$ $\left(^2\Sigma_u^+ + {}^2\Delta_u\right)$ and $^2B_{3g}$ $\left(^2\Pi_g\right)$ symmetries are shown in figure 2 and the corresponding resonance widths for the lowest resonances in the first row of the figure 5. Note that in most cases we have not attempted to track resonances about 10 eV and the resonance widths go to zero when the resonance becomes a bound state. There is one more low-lying resonances for doublet spin symmetry, ^2A_u $\left(^2\Sigma_u^- + {}^2\Delta_u\right)$. This resonance is the same as in the case of $^2B_{1u}$ $\left(^2\Sigma_u^+ + {}^2\Delta_u\right)$ symmetry so we can identify this resonance as $^2\Delta_u$. The quartet spin symmetry resonances and the corresponding resonance widths are given in figures 3–6. Again the widths decrease to zero as the resonances become bound. Data on the high-lying resonance must be considered less reliable.

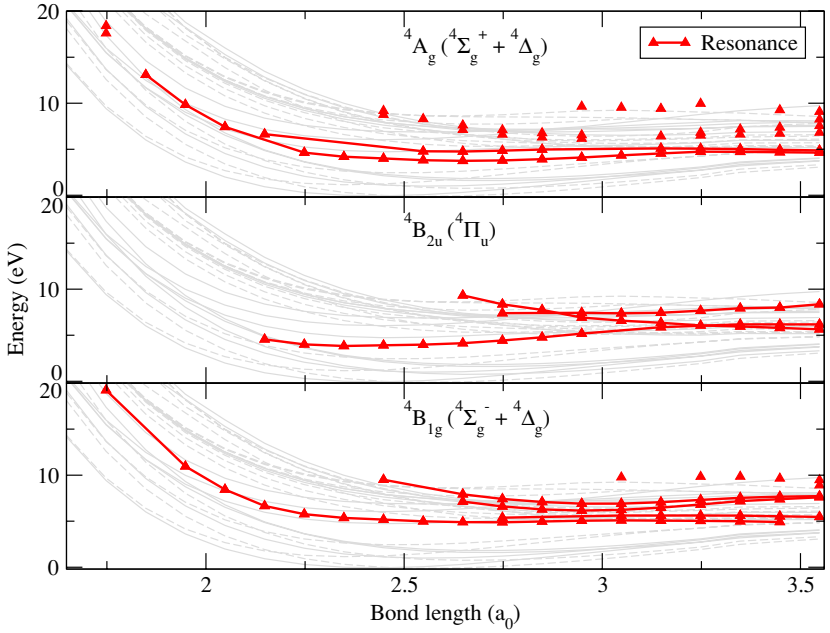

Figure 3. C_2^- resonance energies for ^4A_g ($^4\Sigma_g^+ + {}^4\Delta_g$), $^4B_{2u}$ ($^4\Pi_u$) and $^4B_{1g}$ ($^4\Sigma_g^- + {}^4\Delta_g$) symmetries as a function of the bond length. The energies of the C_2 electronic states used in our calculations are shown in the background: singlet states as solid lines, triplet states as dashed lines.

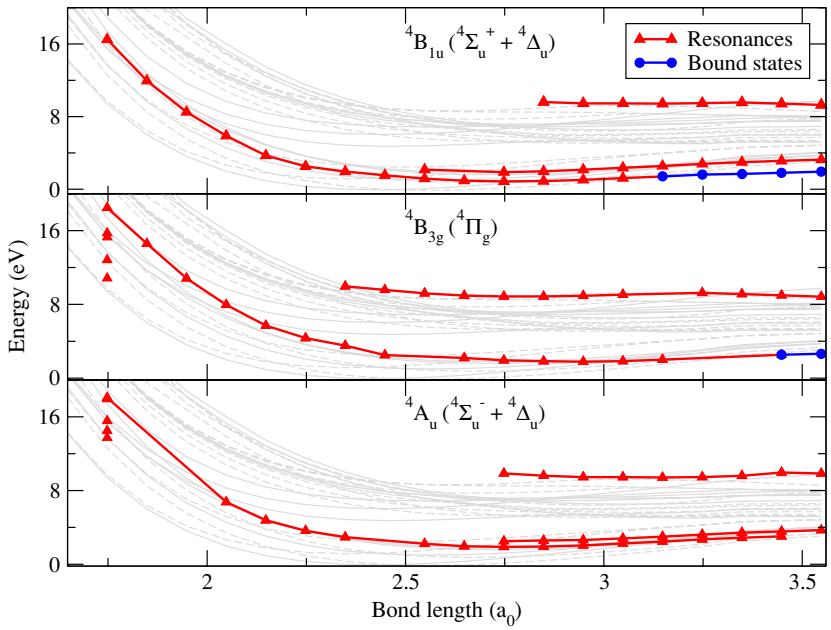

Figure 4. C_2^- bound state and resonance energies for $^4B_{1u}$ ($^4\Sigma_u^+ + {}^4\Delta_u$), $^4B_{3g}$ ($^4\Pi_g$) and ^4A_u ($^4\Sigma_u^- + {}^4\Delta_u$) symmetries as a function of the bond length. The energies of the C_2 electronic states used in our calculations are shown in the background: singlet states as solid lines, triplet states as dashed lines.

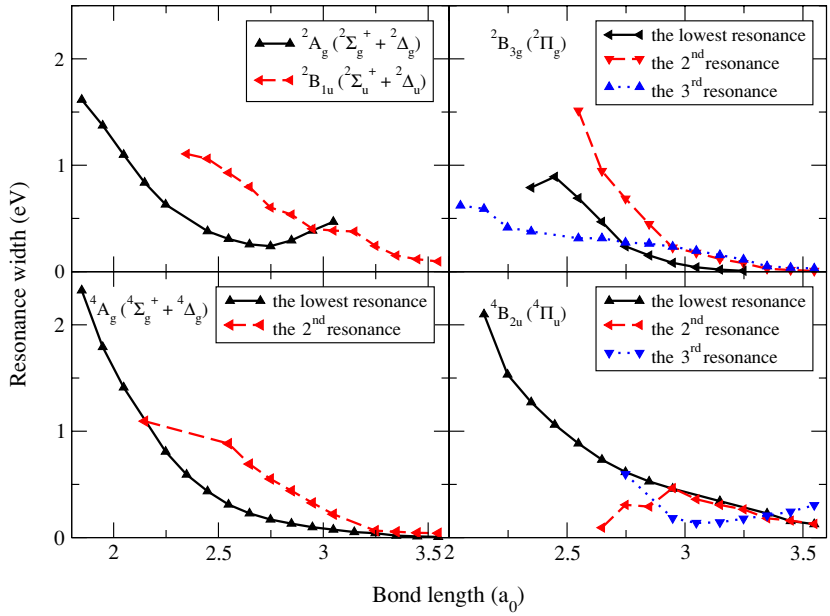

Figure 5. C_2^- resonance widths for ^2A_g ($^2\Sigma_g^+ + {}^2\Delta_g$), $^2B_{1u}$ ($^2\Sigma_u^+ + {}^2\Delta_u$), $^2B_{3g}$ ($^2\Pi_g$), ^4A_g ($^4\Sigma_g^+ + {}^4\Delta_g$) and $^4B_{2u}$ ($^4\Pi_u$) symmetries as a function of the bond length.

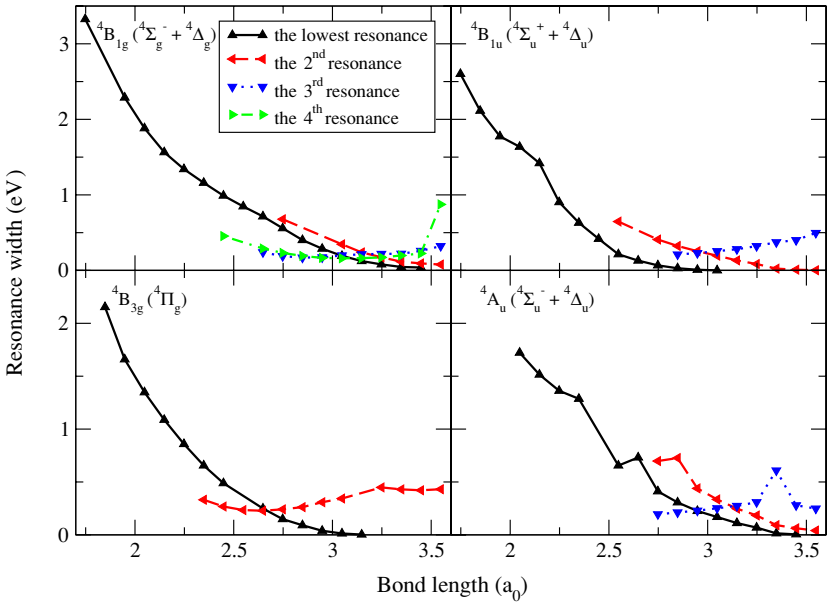

Figure 6. C_2^- resonance widths for $^4B_{1g}$ ($^4\Sigma_g^- + {}^4\Delta_g$), $^4B_{1u}$ ($^4\Sigma_u^+ + {}^4\Delta_u$), $^4B_{3g}$ ($^4\Pi_g$) and ^4A_u ($^4\Sigma_u^- + {}^4\Delta_u$) symmetries as a function of the bond length.

We note that the widths of the resonances do not vary as smoothly with geometry as the positions. There are a number of reasons for this. Firstly, the resonances are characterized

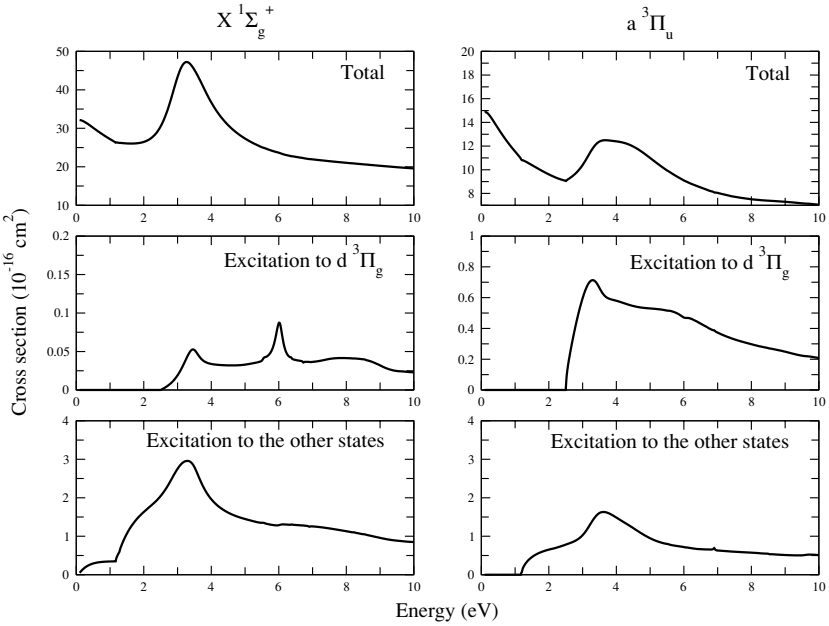

Figure 7. Electronic excitation cross sections from ground state (X $^1\Sigma_g^+$) and first excited state (a $^3\Pi_u$) of C_2 at its equilibrium geometry.

by fitting and experience shows that the resonance width is much more sensitive to details of the fit, and has a larger fitting error, than the position. Secondly, there are many cases where the resonances cross target curves; under these circumstances the resonance width can and does change significantly. Finally, there are several symmetries which have nearby resonances which interact. This is well known to considerably effect the resonance width (Collins *et al* 1986).

4.3. Excitation cross sections

Given the closeness of the X $^1\Sigma_g^+$ and the a $^3\Pi_u$ states, and the fact that the latter is metastable, we consider electronic excitation cross sections from both of these states. Figure 7 gives electron impact cross sections for both of these states at the C_2 equilibrium geometry of $R = 2.448a_0$. These cross sections are only given for electron impact energies up to 10 eV since above this our close-coupling expansion is not complete which can lead to spurious effects.

The top row of graphs presents the fixed-nuclei total cross sections, which are very similar to the elastic cross sections. The total cross sections, and indeed the electronic excitation cross sections also shown, display a pronounced peak at about 3.5 eV; this corresponds to the low-lying $^2\Pi_g$ $\left(^2B_{2g} + {}^2B_{3g}\right)$ and $^2\Delta_u$ $\left(^2B_{1u}\right.$ and $\left.^2A_u\right)$ resonances.

The middle row displays cross sections for the excitation to d $^3\Pi_g$ state. This excited state was selected because the system a $^3\Pi_u$–d $^3\Pi_g$ is well known as Swan bands, whose emission is used to monitor C_2 in plasmas (Stark *et al* 2005, Fantz and Balden 2005). The peak at 6 eV is caused by the ^2A_g $\left(^2\Sigma_g^+ + {}^2\Delta_g\right)$ resonance which is not visible in the other, significantly larger, cross sections reported.

The bottom row gives the cross section for the electron impact excitation to the four electronic states of C_2 lying between the two initial states and d $^3\Pi_g$ state. Information on other electronic excitation cross sections and their behaviour as a function of internuclear separation is available from the authors.

5. Conclusions

We report a study of low-energy electron collisions with the C_2 molecule. Our results confirm that C_2^- has only three truly bound states, all doublets. The $^4\Sigma_u^+$ is found to be a resonance at short bond lengths that becomes bound for internuclear separations larger than $3.1a_0$. Several other low-lying resonance states are also detected. Resonances associated with excited vibrational states of electronically bound states of C_2^- have been observed using high-resolution techniques (Hefter *et al* 1983, Jones *et al* 1980). However, there appears to have been no previous study of electronically excited resonance states. These resonances are important not just because they enhance the elastic and electronically inelastic cross sections but also because they provide the route to dissociative electron attachment and are the dominant means for electron impact vibrational excitation, particularly for a non-polar system such as C_2.

Our calculations also give a wealth of information on the electron impact electronic excitation processes. Such processes play an important role in determining the behaviour of C_2 in plasmas and indeed are probably responsible for emission in the well-known Swan bands in such environments.

References

Abrams M L and Sherrill C D 2004 *J. Chem. Phys.* **121** 9211–9

Andersen L H, Hvelplund P, Kella D, Mokler P H, Pedersen B, Schmidt H T and Vejby-Christensen L 1996 *J. Phys. B: At. Mol. Opt. Phys.* **29** L643–L649

Boggio-Pasqua M, Voronin A I, Halvick P and Rayez J C 2000 *J. Mol. Struct.* **531** 159

Bondybey V E and Brus L E 1975 *J. Chem. Phys.* **63** 2223

Burke P G and Berrington K A (ed) 1993 *Atomic and Molecular Processes, an R-matrix Approach* (Bristol: Institute of Physics Publishing)

Burke P G and Tennyson J 2005 *Mol. Phys.* **103** 2537–48

Christiansen O, Koch H, Jørgensen P and Olsen J 1996 *Chem. Phys. Lett.* **259** 185

Collins L A, Schneider B I, Noble C J, McCurdy C W and Yabushita S 1986 *Phys. Rev. Lett.* **57** 980–3

Dunning T H 1970 *J. Chem. Phys.* **53** 2823

Fantz U and Balden S and ASDEX Upgrade Team 2005 *J. Nucl. Mater.* **337–339** 1087–91

Faure A, Gorfinkiel J D, Morgan L A and Tennyson J 2002 *Comput. Phys. Commun.* **144** 224–41

Gorfinkiel J D, Faure A, Taioli S, Piccarretta C, Halmova G and Tennyson J 2005 *Euro. J. Phys.* D **35** 231–7

Gorfinkiel J D and Tennyson J 2004 *J. Phys. B: At. Mol. Opt. Phys.* **37** L343–L350

Hefter U, Mead R D, Schulz P A and Lineberger W C 1983 *Phys. Rev.* A **28** 1429–39

Herzberg G, Lagerqvist A and Malmberg C 1969 *Can. J. Phys.* **47** 2735

Huber K P and Herzberg G (ed) 1979 *Constants of Diatomic Molecules* (Princeton, NJ: Van Nostrand-Reinhold)

Jones P L, Mead R D, Kohler B E, Rosner S D and Lineberger W C 1980 *J. Chem. Phys.* **73** 4419

Kirby K and Liu B 1979 *J. Chem. Phys.* **70** 893

Morgan L A 1984 *Comput. Phys. Commun.* **31** 419

Morgan L A, Gillan C J, Tennyson J and Chen X 1997 *J. Phys. B: At. Mol. Opt. Phys.* **30** 4087–96

Noble C J and Nesbet R K 1984 *Comput. Phys. Commun.* **33** 399–411

Pedersen B, Djurić N, Jensen M J, Kella D, Safvan C, Schmidt H T, Vejby-Christensen L and Andersen L H 1999 *Phys. Rev.* A **60** 2882

Pedersen H B, Djurić N, Jensen M J, Kella D, Safvan C, Vejby-Christensen L and Andersen L H 1998 *Phys. Rev. Lett.* **81** 5302

Rehfuss B D, Liu D J, Dinelli B M, Jagod M F, Ho W C, Crofton M W and Oka T 1988 *J. Chem. Phys.* **89** 129–37

Rosmus P and Werner H J 1984 *J. Chem. Phys.* **80** 585
Sarpal B K, Branchett S E, Tennyson J and Morgan L A 1991 *J. Phys. B: At. Mol. Opt. Phys.* **24** 3685–99
Stark P, Fantz U and Balden M 2005 *J. Nucl. Mater.* **337–339** 1005–9
Tennyson J 1996 *J. Phys. B: At. Mol. Opt. Phys.* **29** 6185–201
Tennyson J 1997 *Comput. Phys. Commun.* **100** 26–30
Tennyson J and Morgan L A 1999 *Phil. Trans.* A **357** 1161–73
Tennyson J and Noble C J 1984 *Comput. Phys. Commun.* **33** 421–4
Wang R, Zhu Z H and Yang C L 2001 *J. Mol. Struct.(Theochem)* **571** 133–8
Watts D J and Bartlett R J 1992 *J. Chem. Phys.* **96** 6073
Zeitz M, Peyerimhoff S D and Buenker R J 1979 *Chem. Phys. Lett.* **64** 243